

# Effect of chloride substitution on the order–disorder transition in $\text{NaBH}_4$ and $\text{Na}^{11}\text{BD}_4$

---

Jørn Eirik Olsen<sup>1</sup>, Pavel Karen<sup>2</sup>, Magnus H. Sørby<sup>1</sup>, Bjørn C. Hauback<sup>1\*</sup>

<sup>1</sup> Institute for Energy Technology, Physics Department, P.O. Box 40, NO-2027 Kjeller, Norway

<sup>2</sup> University of Oslo, Department of Chemistry, P.O. Box 1033 Blindern, NO-0315 Oslo, Norway

---

\* Corresponding author: E-mail: [bjorn.hauback@ife.no](mailto:bjorn.hauback@ife.no), Phone: +47 63 80 60 78, Fax : +47 63 81 09 20

## ***Abstract***

Phase transition associated with anion disordering over two orientations in  $\text{Na}^{11}\text{BD}_4$  ( $\text{NaBH}_4$ ) and its solid solutions with  $\text{NaCl}$ ,  $\text{Na}^{11}\text{BD}_4)_{1-x}\text{Cl}_x$ , is investigated with powder diffraction (neutron and synchrotron radiation), differential scanning calorimetry and Raman spectroscopy. Upon heating, the transition temperature extrapolated to zero rate of heating is 192.2 K for  $\text{Na}^{11}\text{BD}_4$ ,  $\Delta S = 4.41$  J/molK, hysteresis 1.7 K and the volume increase 0.43%. Thermal parameters of the transition in  $\text{Na}^{11}\text{BD}_4)_{1-x}\text{Cl}_x$  follow a colligative-property model of an ideal solution, with  $x = 0.158(1)$  as the critical concentration at which the ordering interactions and the transition itself are eliminated. On approaching this limit, the tetragonal distortion of the ordered structure decreases somewhat towards the cubic average, and this is associated with a partial disorder of the tetrahedral anions seen by diffraction methods. In fact, a 3% disorder is already present in the pure solvent of the solid solution ( $\text{Na}^{11}\text{BD}_4$ ) at 8 K.

*Keywords:* sodium borohydride, sodium tetrahydridoborate, mechanochemical synthesis, depression of a solid-solvent ordering by a solute, order–disorder transition

## ***Introduction***

$\text{NaBH}_4$  is a possible hydrogen storage material for automotive applications because of its high hydrogen content of 10.7 % by weight [1]. However, it is too stable for on-board storage due to the high decomposition temperature exceeding 500 °C [2]. The stability of the metal tetrahydridoborates, often colloquially referred to as metal borohydrides, in terms of their decomposition temperatures have been suggested to inversely correlate with the Pauling electronegativity of the metal cation [3-5]. The subsequent attempts to

synthesize double-cation metal borohydrides from mixtures of NaBH<sub>4</sub> and various transition metal chlorides by ball milling showed a strong tendency of chloride to substitute for the anions in NaBH<sub>4</sub> [6]. NaBH<sub>4</sub> and NaCl are isostructural and full miscibility is achieved on prolonged ball milling [7, 8].

The solid solution of NaCl in NaBH<sub>4</sub> is interesting on its own. Isoelectronic tetrahedral ions are subject to entropy-driven disordering transitions, such as those revealed by powder neutron diffraction (PND) in solid ND<sub>4</sub>Br [9]. NaBH<sub>4</sub> has just one such transition at 190 K, seen as a lambda point in heat-capacity measurements [10], interpreted by analogy with NH<sub>4</sub><sup>+</sup> as an order–disorder transition of BH<sub>4</sub><sup>−</sup> [11]. It was structurally characterized by Fischer and Züttel [12] as a transition from a *P4<sub>2</sub>/nmc* structure with an ordered arrangement of the tetrahedra into a NaCl-type structure (*Fm-3m*) with the tetrahedra equally disordered over two alternative orientations, resulting in an average arrangement of 8 half-occupied deuterium sites in a cubic configuration around each boron. However, a comprehensive characterization is lacking in terms of the transition order, hysteresis, thermodynamics, and their changes when the interactions behind ordered NaBH<sub>4</sub> are frustrated in the Na(BH<sub>4</sub>)<sub>1−x</sub>Cl<sub>x</sub> solid solutions.

In this study, PND and synchrotron radiation powder X-ray diffraction (SR-PXD) combined with Raman spectrometry are used to establish the thermal evolution of the crystal structure across the phase transition for the sodium borohydride and its solid solutions with NaCl. Differential scanning calorimetry (DSC) reveals how the phase-

transition characteristics are altered by the solid solutions. The colligative properties are shown to be similar to those of an ideal solution freezing and melting.

### ***Experimental***

**Synthesis.** Single-phase solid solutions  $\text{Na}(\text{BH}_4)_{1-x}\text{Cl}_x$  (for  $x = 0.25, 0.50$  and  $0.75$ ) were synthesized from  $\text{NaBH}_4$  (Sigma Aldrich,  $\geq 96\%$ ) and  $\text{NaCl}$  (ABCR, 99.999%) by ball milling for 24 hours under argon in a Fritsch Pulverisette 7 Planetary Mill with grinding jars and balls of hardened stainless steel (ball-to-powder mass ratio 18:1) at a speed of 500 rpm. Single-phase  $\text{Na}({}^{11}\text{BD}_4)_{1-x}\text{Cl}_x$  solid solutions for  $x = 0, 0.10, 0.15, 0.20$  and  $0.25$  were synthesized analogously from  $\text{Na}{}^{11}\text{BD}_4$  (katChem, 99.8%, used due to strong neutron absorption of natural boron and large incoherent scattering of natural hydrogen). The solid solutions for  $x = 0.15$  and  $0.20$  required additional 24 and 48 hours of milling, respectively, to obtain single-phase materials. To avoid contamination from oxygen and air moisture, all samples were handled in MBraun Unilab glove boxes filled with purified Ar ( $< 1\text{ppm O}_2$  and  $\text{H}_2\text{O}$ ).

**Powder X-ray Diffraction (PXD)** was performed to confirm the homogeneity of the solid solution with a Bruker AXS D8 Advance diffractometer in a transmission mode, equipped with a Göbel mirror and a LynxEye<sup>TM</sup> 1D strip detector.  $\text{CuK}_\alpha$  radiation of  $\lambda = 1.5418 \text{ \AA}$  was used on samples in rotating boron-glass capillaries of 0.5 mm in diameter that were filled and sealed under Ar atmosphere.

**DSC** data were collected between 100 and 240 K on  $\text{Na}({}^{11}\text{BD}_4)_{1-x}\text{Cl}_x$  ( $x = 0, 0.10$  and  $0.15$ ) against a heat sink of liquid nitrogen, with a Perkin–Elmer Pyris 1 instrument, on

~30 mg samples precisely weighed and sealed inside the MBraun Unilab glove box into 30  $\mu\text{L}$  aluminum pans. The sample temperature was calibrated on melting pure n-dodecane, m-nitrotoluene, p-nitrotoluene and metallic indium. The transition enthalpy was calibrated on melting of a Perkin–Elmer standard indium. A smooth background was reconstructed from peak-free regions by least-squares fitting with a fifth-order polynomial. The transition enthalpy was evaluated by integrating the heat flow of the peak against the scan time. The corresponding transition entropy was obtained by integrating the heat flow divided by the actual temperature at each scan step (every second). This provides a correct transition-entropy total even if the thermal effect is asymmetric along the temperature axis.

**Combined SR-PXD and Raman data** for  $\text{NaBH}_4$  based samples were collected at the Swiss-Norwegian Beam Line (SNBL, station BM01B) at ESRF, Grenoble, France. The diffractometer is equipped with 6 scintillation detectors mounted with  $1.1^\circ$  separation in  $2\theta$ , each with a secondary monochromator. The measurements were performed in the  $2\theta$  range of  $8$  to  $14.5^\circ$  with the wavelength  $\lambda = 0.50123 \text{ \AA}$  on powder samples in rotating boron glass capillaries of diameter  $0.5 \text{ mm}$ , which were filled and sealed under Ar atmosphere. The data were combined with a  $0.004^\circ$  binning step size. The sample was cooled with a liquid-nitrogen blower from room temperature to  $90 \text{ K}$  at  $3.5 \text{ K/min}$ , and then heated to room temperature at the same rate. A diffraction pattern was obtained every minute giving a temperature resolution of  $3.5 \text{ K}$ . Raman spectra were collected simultaneously on a Renishaw RA 100 Raman analyser, using a  $532 \text{ nm}$  (green)

excitation wavelength in backscattering mode with exposure times between 19 and 59 s and step of  $1.2 \text{ cm}^{-1}$  over a 1000 to  $2700 \text{ cm}^{-1}$  range.

**PND** data were collected for  $\text{Na}({}^{11}\text{BD}_4)_{1-x}\text{Cl}_x$  for  $x = 0, 0.10, 0.15, 0.20$  and  $0.25$  with the PUS instrument at the JEEP II reactor at Kjeller, Norway [13]. Neutrons of wavelength  $\lambda = 1.5556 \text{ \AA}$  were obtained from a Ge (511) vertically focusing monochromator. The samples were sealed in a cylindrical vanadium sample holder of inner diameter 6 mm and mounted in a cryostat (Displex) working with compressed He. Data were collected in the  $2\theta$  range of  $10^\circ$  to  $130^\circ$  at room temperature and 8 K. Temperature evolutions were scanned every 10 K between 10 and 200 K over a  $2\theta$  range of  $27^\circ$  to  $47^\circ$ . Structure refinements were done with the program GSAS [14] and its EXPGUI interface [15]. A shifted Chebyshev function of ten parameters was used to fit the background, and a pseudo-Voigt function of three free parameters to model the Bragg peaks.

### ***Results and discussion***

The structural change at the phase transition in pure  $\text{Na}^{11}\text{BD}_4$  was identified by PND. Rietveld refinements on patterns collected at room temperature and 8 K confirm the respective cubic ( $Fm\bar{3}m$ ) and tetragonal ( $P4_2/nmc$ ) structures reported by Fischer and Züttel [12], while a test with a lower-symmetry space group  $P\bar{4}2_1c$  yields practically no tetrahedral tilt/rotation along  $c$  and no improvement in the  $R_{F2}$  factor. The refined structure parameters and Rietveld fit for the room-temperature structure are in Supplementary Information (Table S1 and Fig. S1); for low-temperature results, see below.



$\text{Na}(\text{BD}_4)_{1-x}\text{Cl}_x$  is almost entirely disrupted, except for a few limited regions that are still ordered and able to absorb some heat for an entropy increase upon disordering.

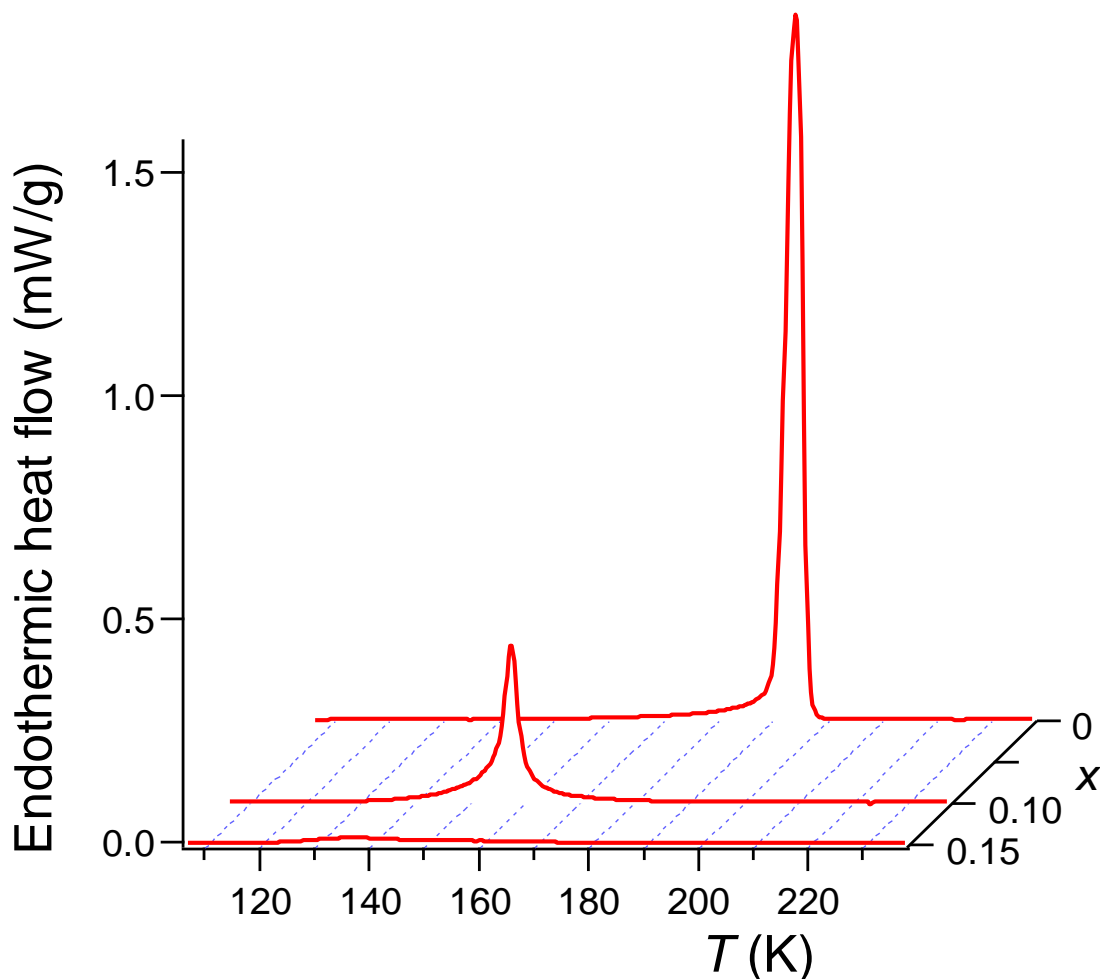


**Fig. 2. Endothermic effect upon heating  $\text{Na}(\text{BD}_4)_{1-x}\text{Cl}_x$  through the order–disorder transition.**

The cyclic DSC scans in Fig. 3 and Fig. 4 illustrate a small hysteresis of the phase transition due to weak interactions between the  $^{11}\text{BD}_4^-$  tetrahedra. The ordering in the pure  $\text{Na}^{11}\text{BD}_4$  sample proceeds in two closely coupled steps separated by  $\sim 2$  K (Fig. 3) that develop upon thermal cycling, probably upon competition between two close subsets of the tetrahedral disorder. In contrast, a single peak is observed for the  $\text{Na}(\text{BD}_4)_{1-x}\text{Cl}_x$  solid solutions (Fig. 4 and Supplementary Information). Extrapolations to the zero scan speed (Fig. 5) show that the hysteresis in pure  $\text{Na}^{11}\text{BD}_4$  is 1.7 K and decreases to 1.3 K

for  $x = 0.10$  and  $\sim 1.0$  K for  $x = 0.15$  (Supplementary Information) as the ordering interactions weaken in the regions of remaining order.

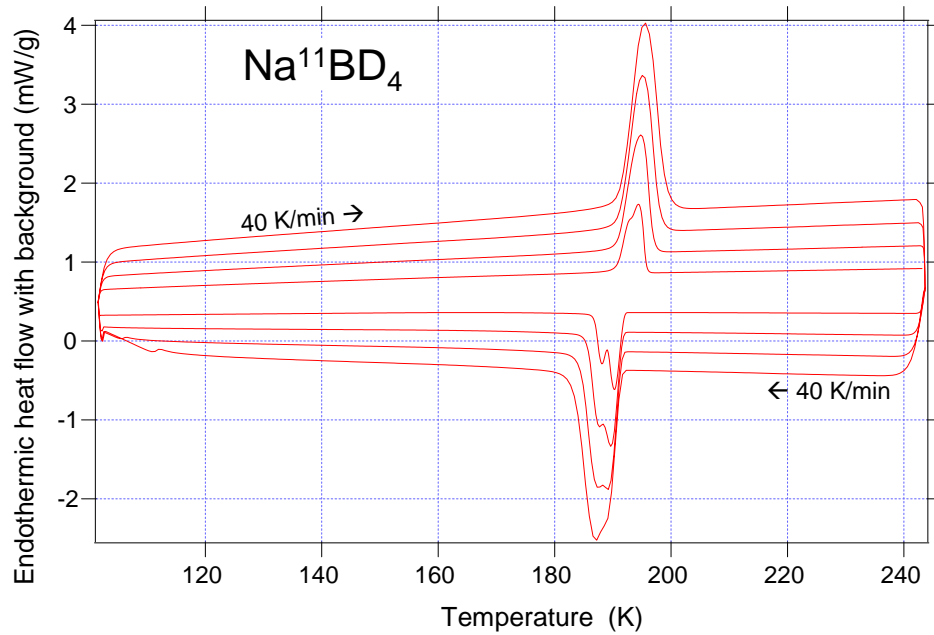


Fig. 3. DSC of  $\text{Na}^{11}\text{BD}_4$  upon heating and cooling at decreasing rates of 40, 30, 20 and 10 K/min.

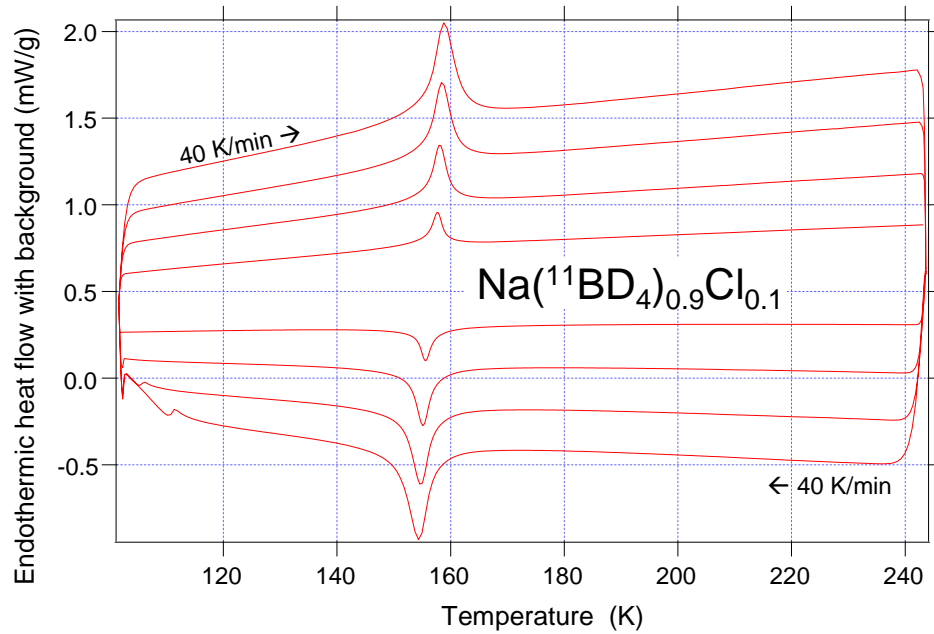
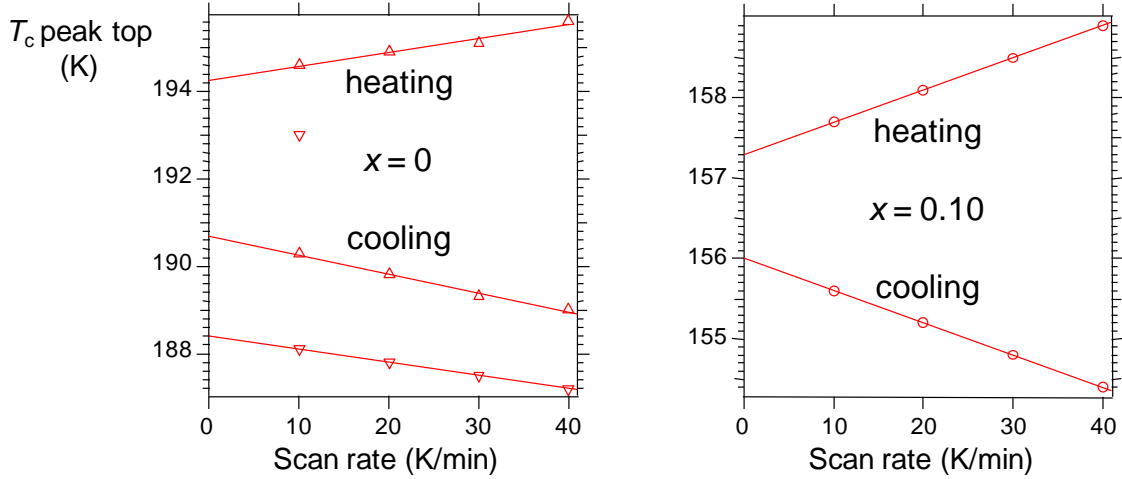


Fig. 4. DSC of  $\text{Na}^{(11}\text{BD}_4)_{0.9}\text{Cl}_{0.10}$  upon heating and cooling at rates decreasing from 40, 30, 20 to 10 K/min.



**Fig. 5.** Extrapolations of heating and cooling scans to zero scan rate for  $\text{Na}(\text{BD}_4)_{1-x}\text{Cl}_x$ . The up and down triangle symbols on left refer to the DSC peak doublets in Fig. 3.

**Table 1.** Thermal parameters evaluated upon heating through the disordering transition at 20 K/min.

$x$	$\Delta H$ (kJ/mol)	$\Delta S$ (J/molK)	Peak center (K)
0.00	0.851	4.412	192.8
0.10	0.294	1.871	157.0
0.15	0.046	0.323	144.3

The entropy change upon the order–disorder transition in the pure  $\text{Na}^{11}\text{BD}_4$  solvent is  $\Delta S = 4.41$  J/molK. This represents 76% of the theoretical value  $R\ln 2 = 5.762$  J/molK ( $R$  is the molar gas constant) upon disordering one mole of ordered tetrahedra over two orientations. Increasing solute concentration decreases the thermal parameters (Table 1). A colligative-property approach is adopted [16] to tie together the transition enthalpy, entropy and critical temperature as a function of the NaCl solute fraction  $x$  in the  $\text{Na}(\text{BD}_4)_{1-x}\text{Cl}_x$  solid solutions. Assuming ideal solution and a temperature-independent enthalpy of the pure solvent, the phase-transition temperature  $T_c(x) = \Delta H(x)/\Delta S(x)$  decreases with increasing molar fraction  $x$  of the solute as:

$$\Delta H(x)/\Delta S(x) = \Delta H(0)/[\Delta S(0) - R\ln(1-x)] \quad (1)$$

where  $\Delta H(0)$  is the enthalpy at  $x = 0$ . The transition-enthalpy decrease is considered linear:

$$\Delta H(x) = \Delta H(0) (1 - x/x_{\text{end}}) \quad (2)$$

where  $x_{\text{end}}$  is the  $x$  when  $\Delta H(x)$  becomes zero. The transition enthalpies and entropies of the solid solutions as a function of  $x$  (Table 1) were fitted by least squares to satisfy  $\Delta H(x)$  of Equation (2) and simultaneously  $\Delta S(x)$  obtained from (1) upon substituting for  $\Delta H(x)$  from (2). The obtained fit parameters were  $\Delta H(0) = 0.845(41)$  kJ/mol,  $\Delta S(0) = 4.39(4)$  J/molK and  $x_{\text{end}} = 0.158(1)$ . The graphical representation of this result is in Fig. 6. Comparison on right of Fig. 6 of the calculated  $T_c$  with the experimental peak-center temperatures shows that the results are mutually consistent, but suggests a small deviation from ideality.

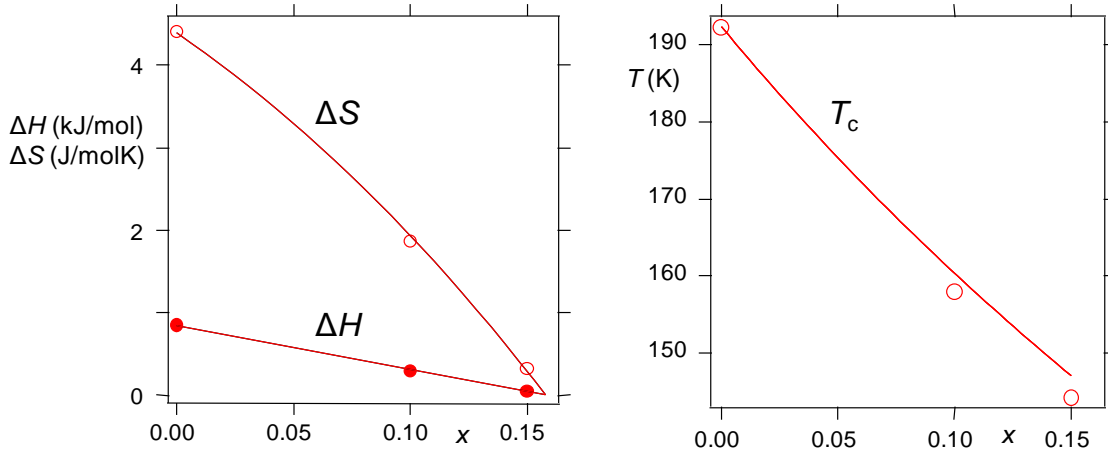


**Fig. 6. Colligative properties for ideal-solution model for the phase-transition temperature depression in  $\text{Na}(\text{BD}_4)_{1-x}\text{Cl}_x$  (lines are fitted, see text; points are experimental).**

Practically the same phase-transition temperatures are seen for the evolution of the deuterium ordering peaks (102 and 201) in the PND data for  $\text{Na}^{11}\text{BD}_4$ , plotted in Fig. 7. From the same data, a volume increase of 0.43 % upon heating through the transition is

evaluated from a linear fit of the low- and high-temperature PND unit-cell volumes as a function of temperature (0.4% is reported for NaBH<sub>4</sub> [17]). Clapeyron equation yields the pressure change of the transition temperature: With  $\Delta V = 1.45(24) \cdot 10^{-8} \text{ m}^3$  and  $\Delta S = 4.39(4) \text{ J/molK}$  from the colligative fit,  $dP/dT_c = 3.04(54) \cdot 10^7 \text{ Pa/K}$ . This suggests that in Na<sup>11</sup>BD<sub>4</sub> at 3 GPa of pressure, this transition would occur at room temperature. Or at 4 GPa when theoretical  $\Delta S = R \ln 2 = 5.762 \text{ J/molK}$  is considered. A high-pressure study [18] of NaBH<sub>4</sub> thermal conductivity indeed shows the transition temperature increasing by ~50 K as the pressure reaches 2 GPa.

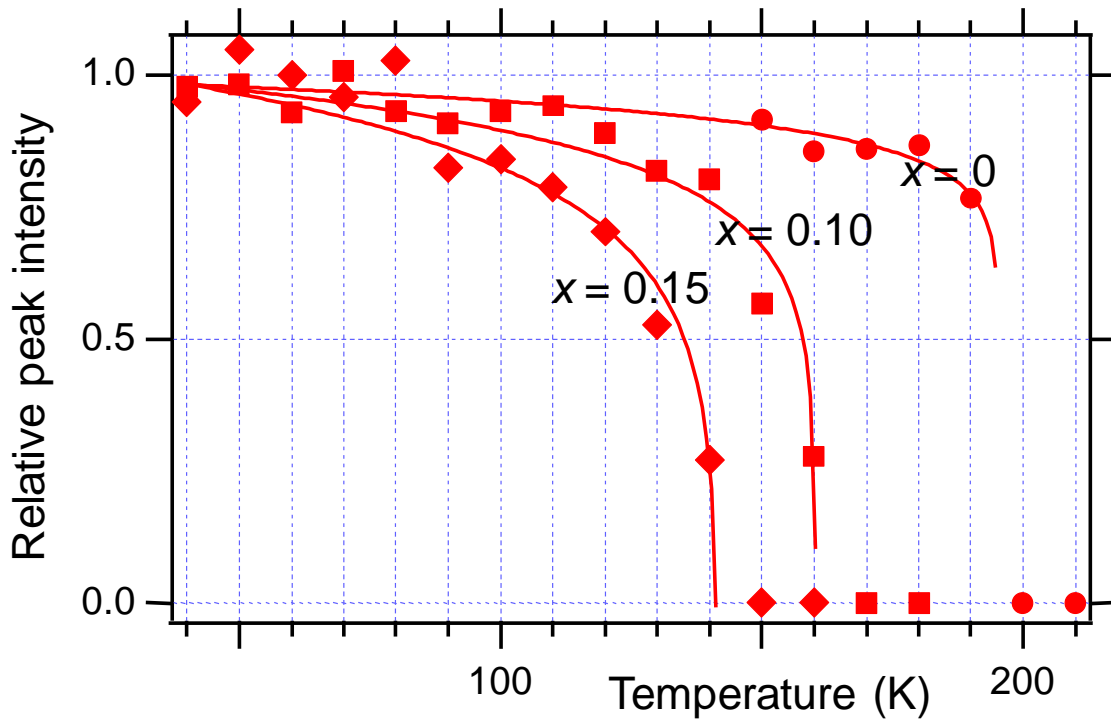
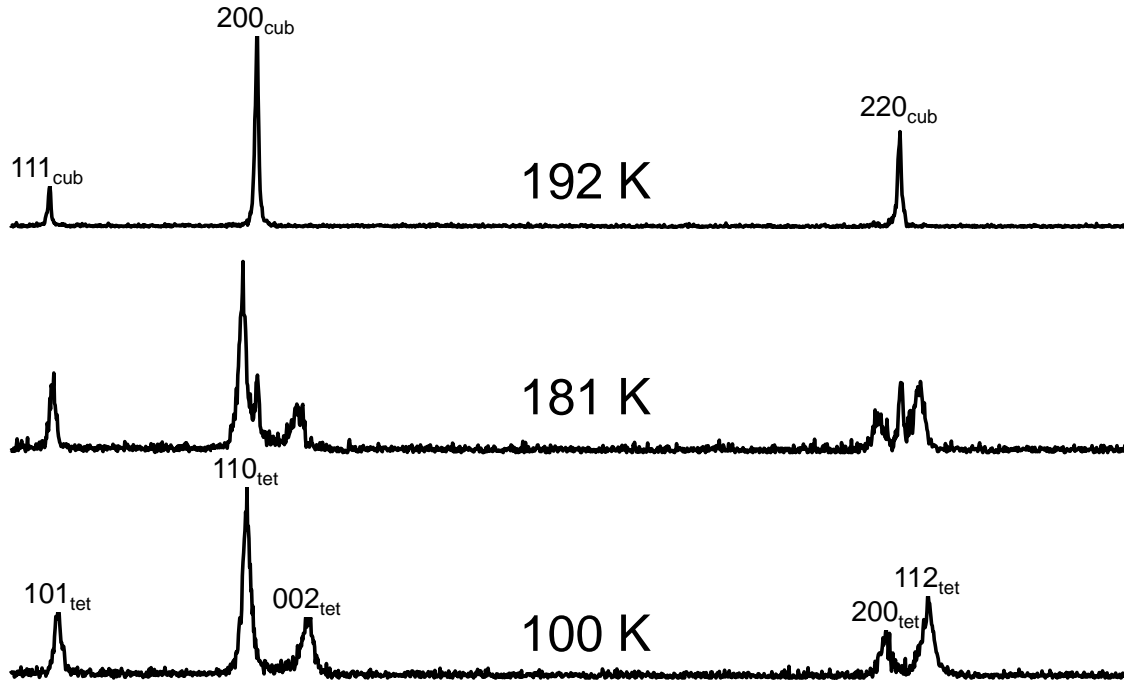


Fig. 7. Vanishing superstructure PND reflections (102 and 201 summed, Fig. 10) of Na(<sup>11</sup>BD<sub>4</sub>)<sub>1-x</sub>Cl<sub>x</sub> upon heating. The intensities are normalized to the values found at 8 K.

An entirely analogous transition is observed in NaBH<sub>4</sub> by SR-PXD, except that the transition temperatures are lower than those for Na<sup>11</sup>BD<sub>4</sub> due to isotope effect. The phase transition is manifested by a two-phase range that occurs between 180 and 190 K, Fig. 8.

The simultaneously collected Raman spectra in Fig. 9, assigned as in Ref. [19], show that the resolution of the Raman absorptions increases upon ordering, in particular for the strongest symmetric stretching mode  $\nu_1$ . As expected, no phase transition is seen in  $\text{Na}(\text{BH}_4)_{1-x}\text{Cl}_x$  for  $x = 0.25, 0.5$  and  $0.75$ .



**Fig. 8.** Comparison of SR-PXD patterns ( $8$  to  $14.5^\circ 2\theta$ ) upon heating  $\text{NaBH}_4$  of the tetragonal (bottom) and cubic (top) phases, with a range of coexistence (middle) at the transition between  $180$  and  $190$  K.

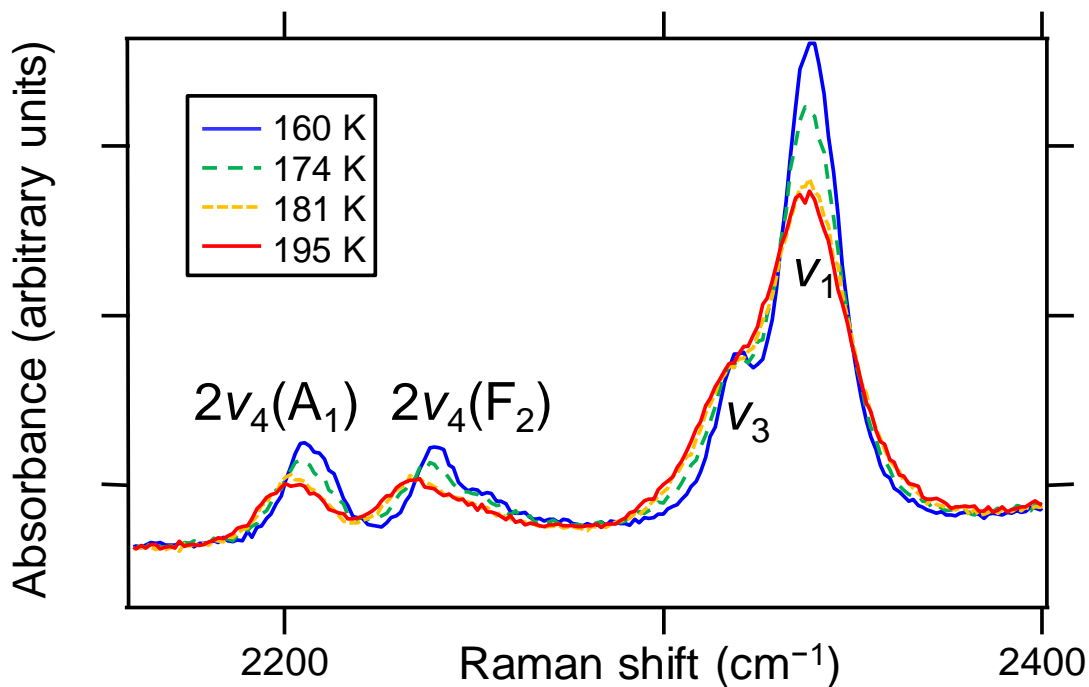
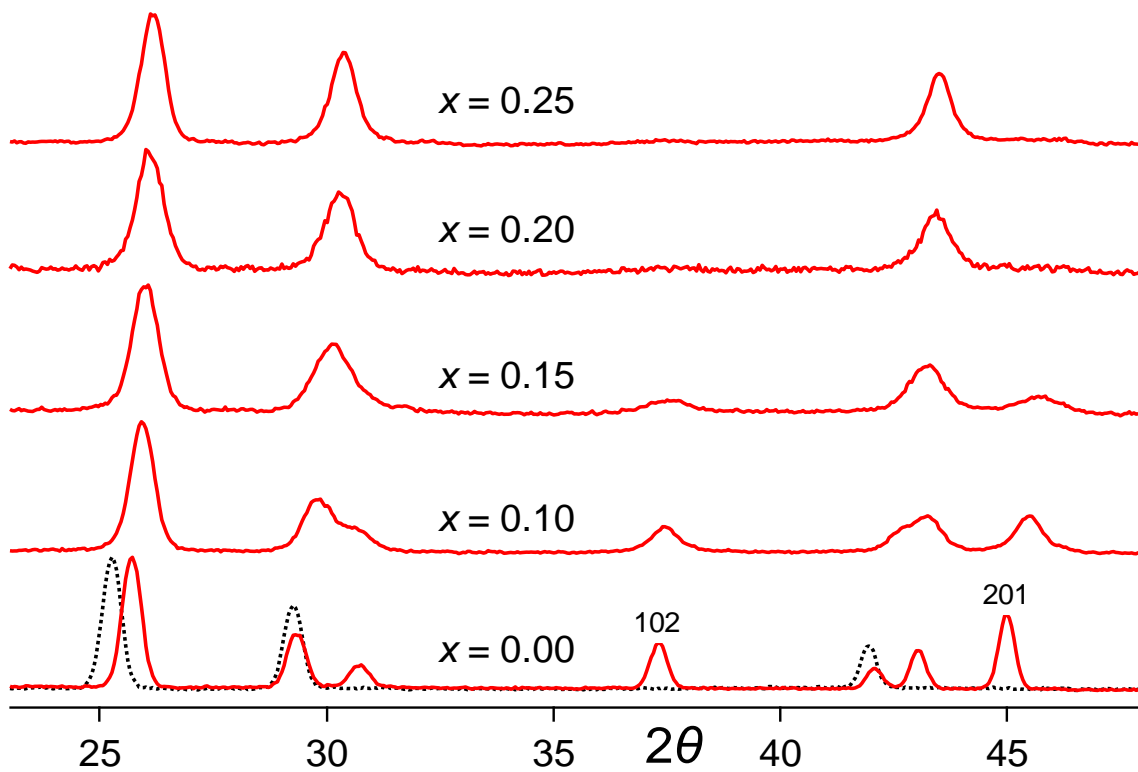


Fig. 9. Raman spectra at selected temperatures upon heating  $\text{NaBH}_4$ .

The PND patterns collected at 8 K also illustrate the interference of the NaCl solute with the ordered low-temperature structure in  $\text{Na}({}^{11}\text{BD}_4)_{1-x}\text{Cl}_x$  (Fig. 10), which is no longer observed at 8 K for the substitution level  $x = 0.20$  and higher. The increasing degree of disorder in the long-range ordered phase at 8 K is apparent from the refined unit-cell parameters as the difference between  $c_{\text{tet}}$  and  $\sqrt{2}a_{\text{tet}}$  decreases with increasing  $x$  (Fig. 11) to become zero at cubic symmetry.



**Fig. 10.** PND patterns of  $\text{Na}^{(11}\text{BD}_4)_{1-x}\text{Cl}_x$  at 8 K. Increasing concentration  $x$  of the NaCl solute frustrates ordering in the  $\text{Na}^{11}\text{BD}_4$  solvent, as apparent from decreasing intensity of ordered-structure peaks 201 and 102 identified on the  $x = 0.00$  plot, where also the room-temperature pattern is shown for comparison with a dashed line.

**Table 2 Results of Rietveld refinements from PND patterns of  $\text{Na}^{(11}\text{BD}_4)_{1-x}\text{Cl}_x$  ( $x = 0, 0.10, 0.15$ ) at 8 K, in the space group  $P4_2/nmc$ . Standard deviations of refined values are in brackets.**

	$\text{Na}^{11}\text{BD}_4$	$\text{Na}^{(11}\text{BD}_4)_{0.90}\text{Cl}_{0.10}$	$\text{Na}^{(11}\text{BD}_4)_{0.85}\text{Cl}_{0.15}$
Unit-cell parameters [Å]	$a = 4.329(1)$ $c = 5.868(1)$	$a = 4.282(1)$ $c = 5.886(1)$	$a = 4.249(1)$ $c = 5.900(1)$
Unit-cell volume [Å <sup>3</sup> ]	109.98(1) Å <sup>3</sup>	107.90(2)	106.52(2)
Calculated density [g/cm <sup>3</sup> ]	1.270	1.345	1.388
$R_{F2}$	0.0632	0.0619	0.0813
Na (2a) $x y z$	$\frac{3}{4} \frac{1}{4} \frac{3}{4}$	$\frac{3}{4} \frac{1}{4} \frac{3}{4}$	$\frac{3}{4} \frac{1}{4} \frac{3}{4}$
$U_{iso}$ [Å]	0.0010(6)	0.0025(5)	0.0090(7)
Occupancy	1	1	1
B (2b) $x y z$	$\frac{3}{4} \frac{1}{4} \frac{3}{4}$	$\frac{3}{4} \frac{1}{4} \frac{3}{4}$	$\frac{3}{4} \frac{1}{4} \frac{3}{4}$
$U_{iso}$ [Å]	0.0011(6)	0.0057(3)	0.0018(3)
Occupancy	1	0.90	0.85
Cl (2b) $x y z$	-	$\frac{3}{4} \frac{1}{4} \frac{3}{4}$	$\frac{3}{4} \frac{1}{4} \frac{3}{4}$
$U_{iso}$ [Å]	-	0.025(3)	0.045(3)
Occupancy	-	0.10	0.15
D1 (8g) $x y z$	$\frac{1}{4} 0.9797(2) 0.8689(2)$	$\frac{1}{4} 0.9825(3) 0.8689(2)$	$\frac{1}{4} 0.9828(4) 0.8658(4)$
$U_{iso}$ [Å]	0.0207(7)	0.0303(3)	0.0365(4)
Occupancy	0.984(2)	0.817(1)	0.692(2)
D2 (8g) $x y z$	$\frac{1}{4} y(\text{D1}) 0.6311(2)^a$	$\frac{1}{4} y(\text{D1}) 0.6311(2)^a$	$\frac{1}{4} y(\text{D1}) 0.6342(4)^a$
$U_{iso}$ [Å]	$= U_{iso}(\text{D1})$	$= U_{iso}(\text{D1})$	$= U_{iso}(\text{D1})$
Occupancy	0.016(2) <sup>b</sup>	0.083(1) <sup>b</sup>	0.158(2) <sup>b</sup>
Degree of disorder [%] <sup>c</sup>	3	18	37

<sup>a</sup> Constrained to  $z(\text{D2}) = 1.5 - z(\text{D1})$ , <sup>b</sup> Constrained to  $\text{Occ}(\text{B}) - \text{Occ}(\text{D1})$ , <sup>c</sup>  $200 \times \text{Occ}(\text{D2}) / (\text{Occ}(\text{D1}) + \text{Occ}(\text{D2}))$ .

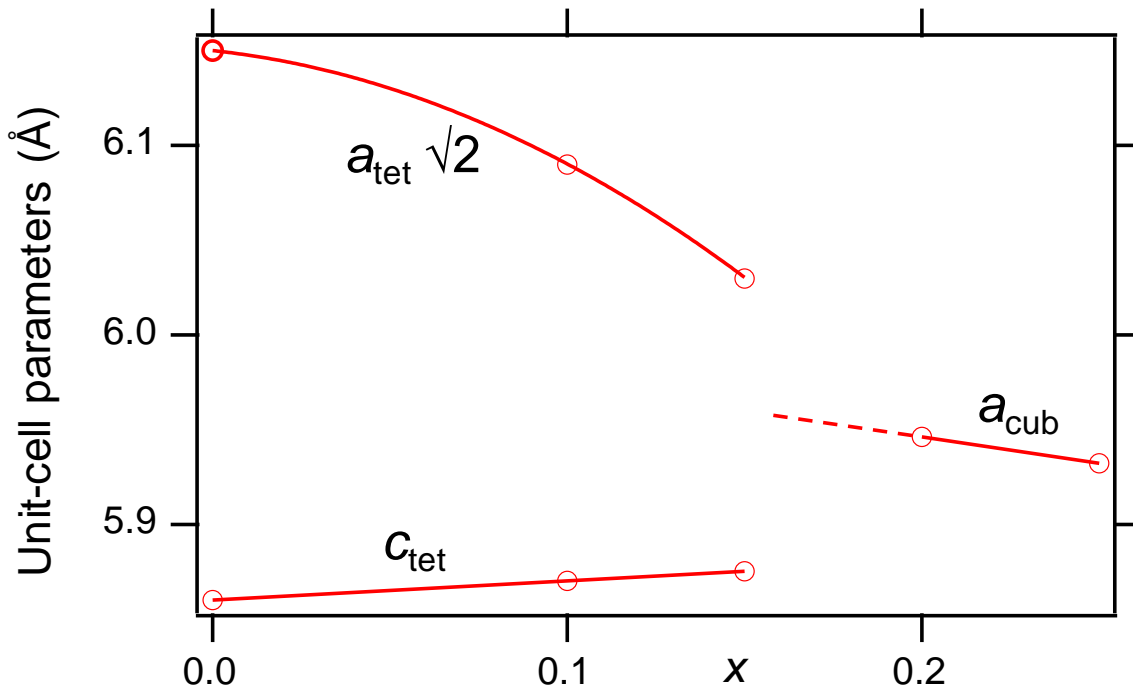


**Fig. 11. Unit-cell parameters of the  $\text{Na}^{(11}\text{BD}_4)_{1-x}\text{Cl}_x$  solid solution as determined by PND at 8 K.**

The gradual approach, even at 8 K, of the tetragonal order of the borohydride anions towards the cubic disorder upon increasing frustration by the spectator anion of the solute

must have a structural explanation. Indeed, the intensities of the ordering peaks are calculated too high in fully ordered structure models of the Cl-substituted phases. The implied disorder was modelled by introducing an additional deuterium site, D2, for  $\text{BD}_4^-$  orientation analogous to that seen at room temperature. The occupancies of the two deuterium sites were refined with the constraint that their sum should equal the nominal occupancy  $1-x$  of the boron site. The refined parameters are given in Table 2 and the Rietveld fits are shown in Fig. 12 and Fig.S2–S5 (Supplementary Information). It turns out that even chloride-free  $\text{Na}^{11}\text{BD}_4$  has a detectable degree of  $^{11}\text{BD}_4^-$  disorder of 3%. The disorder increases to 18% and 37% in  $\text{Na}(^{11}\text{BD}_4)_{0.90}\text{Cl}_{0.10}$  and  $\text{Na}(^{11}\text{BD}_4)_{0.85}\text{Cl}_{0.15}$ , respectively.  $\text{Na}(^{11}\text{BD}_4)_{0.80}\text{Cl}_{0.20}$  and  $\text{Na}(^{11}\text{BD}_4)_{0.75}\text{Cl}_{0.25}$  are 100% disordered since the sites “D1” and “D2” are equivalent under the  $Fm-3m$  space-group symmetry (Table S2 and S3 in Supplementary Information).

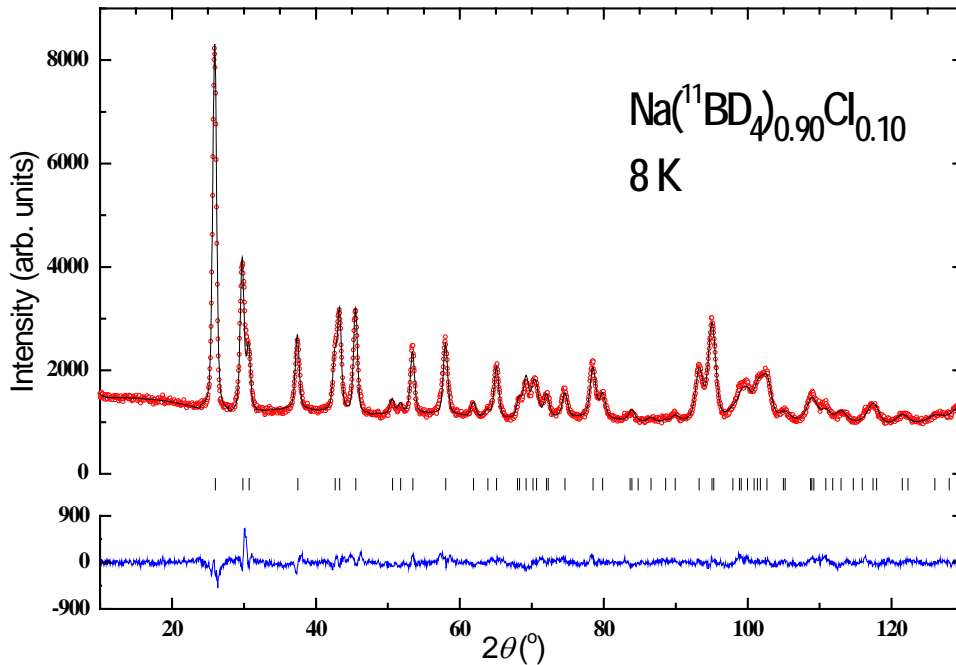


**Fig. 12** Rietveld fit showing experimental (black solid line) and calculated (red circles) PND profile of  $\text{Na}(^{11}\text{BD}_4)_{0.90}\text{Cl}_{0.10}$  at 8 K. The blue line is the difference plot. Bragg peaks are marked with vertical ticks;  $R_{F2} = 0.0619$ ;  $\lambda = 1.5556 \text{ \AA}$ .

## ***Conclusions***

Refinements from PND data confirm the structural models of Fischer and Züttel [12] for  $\text{Na}^{11}\text{BD}_4$  of the  $P4_2/nmc$  symmetry at 8 K and  $Fm\bar{3}m$  at room temperature, but with a small degree of residual orientational disorder (3%) even at 8 K. The transition between these two structures occurs at 192.2 K upon heating at a zero rate. The entropy increase associated with the  $^{11}\text{BD}_4^-$  disordering in pure  $\text{Na}^{11}\text{BD}_4$  is  $\Delta S = 4.41 \text{ J/molK}$ , or 76% of the theory value  $R\ln 2 = 5.762 \text{ J/molK}$ . The transition has a small hysteresis of 1.7 K and proceeds upon a volume increase of 0.43 % upon heating, similar to 0.4% reported for  $\text{NaBH}_4$  [17]. Together with the observed two-phase presence within the transition range of temperatures, these facts suggest this transition to be of the first order, in conformity with the lambda shape for the heat capacity in Ref. [10] .

In the solid solutions with NaCl, the weak interactions behind the ordered tetragonal superstructure of the  $\text{BH}_4^-/^{11}\text{BD}_4^-$  anions are increasingly frustrated by the chloride ions uninvolved in the ordering interactions. The profound decrease in the transition enthalpy, entropy and a moderate decrease in the transition temperature follow roughly the colligative-property model of the freezing point for an ideal liquid solution. The experimental data extrapolate to the NaCl solute concentration of  $x = 0.158(1)$ , at which the frustration overcomes the communication between the borohydride anions so that their ordering is no longer possible. Approaching this limit, the tetragonal distortion of the ordered structure decreases somewhat towards the cubic average. Structurally, this is associated with a partial disorder of the tetrahedral anions increasing from the nearly full

long-range order of the pure solvent towards the full disorder over two orientations as seen at room temperature.

### ***Acknowledgement***

JEO, MHS and BCH acknowledge the Research Council of Norway for financial support through the FRIENERGI program and the staff of SNBL at ESRF for helpful assistance.

### ***References***

- [1] L. Schlapbach, A. Züttel, *Nature* 414 (2001) 353–358.
- [2] P. Martelli, R. Caputo, A. Remhof, P. Mauron, A. Borgschulte, A. Züttel, *Journal of Physical Chemistry C* 114 (2010) 7173–7177.
- [3] G.N. Schrauzer, *Naturwissenschaften* 42 (1955) 438–438.
- [4] Y. Nakamori, K. Miwa, A. Ninomiya, H.W. Li, N. Ohba, S.I. Towata, A. Zuttel, S.I. Orimo, *Physical Review B* 74 (2006) 045126/1–9.
- [5] Y. Nakamori, H.W. Li, K. Kikuchi, M. Aoki, K. Miwa, S. Towata, S. Orimo, *Journal of Alloys and Compounds* 446 (2007) 296–300.
- [6] I. Llamas-Jansa, N. Aliouane, S. Deledda, J.E. Fonnelløp, C. Frommen, T. Humphries, K. Lieutenant, S. Sartori, M.H. Sørby, B.C. Hauback, *Journal of Alloys and Compounds* 530 (2012) 186–192.
- [7] J.E. Olsen, M.H. Sørby, B.C. Hauback, *Journal of Alloys and Compounds* 509 (2011) L228–L231.
- [8] D.B. Ravnsbæk, L.H. Rude, T.R. Jensen, *Journal of Solid State Chemistry* 184 (2011) 1858–1866.
- [9] H.A. Levy, S.W. Peterson, *Journal of the American Chemical Society* 75 (1953) 1536–1542.
- [10] H.L. Johnston, N.C. Hallett, *Journal of the American Chemical Society* 75 (1953) 1467–1468.
- [11] W.H. Stockmayer, C.C. Stephenson, *Journal of Chemical Physics* 21 (1953) 1311–1312.
- [12] P. Fischer, A. Züttel, *Materials Science Forum* 443–444 (2004) 287–290. DOI: 210.4028/www.scientific.net/MSF.4443-4444.4287.
- [13] B.C. Hauback, H. Fjellvåg, O. Steinsvoll, K. Johansson, O.T. Buset, J. Jørgensen, *Journal of Neutron Research* 8 (2000) 215–232.
- [14] A.C. Larson, R.B. von Dreele, *General Structure Analysis System (GSAS)*, in, Los Alamos National Laboratory Report, Los Alamos, 2004.
- [15] B.H. Toby, *Journal of Applied Crystallography* 34 (2001) 210–221.
- [16] P. Karen, *Journal of Solid State Chemistry* 177 (2004) 281–292.
- [17] O.A. Babanova, A.V. Soloninin, A.P. Stepanov, A.V. Skripov, Y. Filinchuk, *Journal of Physical Chemistry C* 114 (2010) 3712–3718.
- [18] B. Sundqvist, O. Andersson, *Physical Review B* 73 (2006) 092102/1–3.
- [19] G. Renaudin, S. Gomes, H. Hagemann, L. Keller, K. Yvon, *Journal of Alloys and Compounds* 375 (2004) 98–106.